The Single-crystal Electronic and Electron Spin Resonance Spectra of Copper(II) Doped Bis(2,2'-bipyridyl)nitritozinc(II) Nitrate and Bis(2,2'-bipyridyl)nitritocopper(II) Tetrafluoroborate: A Fluxional $CuN_2N'_2O_2$ Chromophore

By **William Fitzgerald, Brigid Murphy, Suresh Tyagi, Bernadette Walsh, Andrew Walsh,** and **Brian Hathaway,*** The Chemistry Department, University College, Cork, Ireland

The single-crystal e.s.r. spectra and polarised electronic spectra of the copper(II) doped $[Zn(bipy)_2(ONO)][NO_3]$ system are shown to be closely comparable to those previously reported for $[Cu(bipy)_2(ONO)][NO_3]$. The observation of more than four copper hyperfine lines in the single-crystal e.s.r. spectrum measured in the approximate *bc* plane is consistent with a two-dimensional misalignment of the $CuN_2N'_2O_2$ chromophore and the temperature variability of the *g* and *A* factors are consistent with a two-dimensional fluxional model of the $CuN_2N'_2O_2$ chromophore with a distorted square-pyramidal 4 + 1 + 1* structure and *not* with static disorder. This suggests that the structures of $[Cu(bipy)_2(ONO)][NO_3]$ and $[Cu(bipy)_2(ONO)][BF_4]$ are not genuine static stereochemistries of the copper(II) ion, but arise as a consequence of the fluxional model and are best referred to as pseudo *cis* distorted-octahedral structures. The electronic properties of 0.1—100% copper(II) doped $[Zn(bipy)_2(ONO)][NO_3]$ are shown to be independent of the copper(II) concentration, and this suggests that the structure of the doped $CuN_2N'_2O_2$ chromophore is independent of the structure of the $ZnN_2N'_2O_2$ chromophore of the zinc host lattice, but correlates with the known structure of the $[Cu(bipy)_2(ONO)][NO_3]$ complex, an example of the Non-co-operative Jahn–Teller Effect. The electronic reflectance spectrum of $[Cu(bipy)_2(ONO)][BF_4]$ is closely comparable to that of the nitrate, despite having a significantly different, (4 + 1 + 1*) type, fluxional CuN_4O_2 chromophore structure.

THE *cis*-distorted octahedral CuN_4O_2 chromophore [1] of $[Cu(bipy)_2(ONO)][NO_3]$ (bipy = 2,2'-bipyridyl) (1) (Figure 1) was for ten years the only example known for this stereochemistry of the copper(II) ion. The recent crystal structure determination [2] of $[Cu(bipy)_2(ONO)][BF_4]$ (2) has produced a second example of this structure, but one involving a more asymmetrically bonded ONO^- anion. In order to understand the different structures observed in these two cation distortion isomers [3] the electronic properties of (2) are reported along with the single-crystal electronic properties of the $[Cu(bipy)_2(ONO)]^+$ cation doped in $[Zn(bipy)_2(ONO)][NO_3]$ (3) as a diamagnetic host lattice,[2] over the concentration range 0.1—100%.

EXPERIMENTAL

Preparation.—The copper(II) doped crystals of (3) were prepared as previously reported [1] for (1), using the appropriate stoicheiometric amounts of $Cu[NO_3]_2 \cdot 3H_2O$ and $Zn[NO_3]_2 \cdot 6H_2O$; large crystals were obtained if methanol, rather than ethanol, was used as a solvent. In the copper doped complex (3) the Cu : Zn ratio was determined by atomic absorption analysis; complex (2) was prepared as previously reported.[2]

Electronic Properties.—These were recorded as previously described.[4,5] Figure 2 reports the electronic reflectance spectra of 1—100% copper(II) doped $[Zn(bipy)_2(ONO)][NO_3]$ and Figure 3, the corresponding polarised single-crystal spectra.[5] Figure 4(*a*) shows the polycrystalline e.s.r. spectra of 0.1—100% copper doped complex (3), Figure 4(*b*), the effect of temperature on the polycrystalline e.s.r. spectrum of 0.1% copper doped (3), Figure 4(*c*) and (*d*), the polycrystalline e.s.r. spectra of (1) and (2), respectively, at room and liquid-nitrogen temperature, and Figure 4(*e*) shows the nitrogen hyperfine on the single-crystal e.s.r. spectrum of 0.1% copper doped (3) at liquid-nitrogen temperature. Figure 5(*a*) shows the crystal morphology [3] of the 0.1% copper doped (3) system and Figure 5(*b*)—(*d*) shows the single-crystal e.s.r. rotation spectra measured in the *ac* plane, the *b* axis/$g_{min.}$ plane, and the Zn, N(2), N(4), O(1), O(2) plane (liquid-nitrogen and room temperatures) respectively. Table 1 lists the electronic reflectance spectra

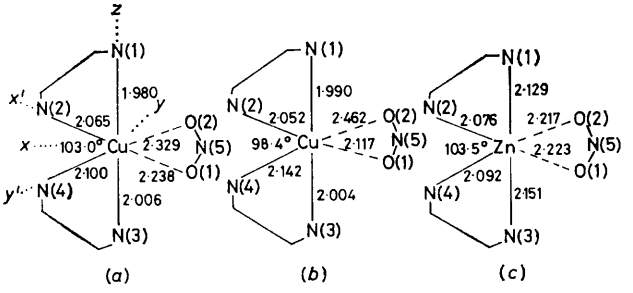

FIGURE 1 The local molecular structures of (*a*) $[Cu(bipy)_2(ONO)][NO_3]$ (1), (*b*) $[Cu(bipy)_2(ONO)][BF_4]$ (2), and (*c*) $[Zn(bipy)_2(ONO)][NO_3]$ (3)

of some $[Cu(bipy)_2(OXO)]Y$ complexes, Table 2 lists the single-crystal e.s.r. data for (1) and copper doped (3) at room temperature and at liquid-nitrogen temperature, and Table 3 lists the unit-cell data [1,2] for (1) and (3).

RESULTS

Electronic Spectra.—The electronic reflectance spectra of (1), (2), and of copper(II) doped (3) consist [3] of two broad peaks of comparable intensity (Figure 2) at 9 500 and 14 600—15 000 cm^{-1}. The spectra show only a small variation with the anion present (Table 1), and a negligible variation [6] with the copper(II) concentration for 0.1—100% copper doped complex (3). This comparability of the electronic spectra is also present in the polarised single-crystal electronic spectra [3] of 1—100% copper(II) doped (3) and suggests that the underlying stereochemistry of the CuN_4O_2 chromophore in (1) does not differ significantly [6] from that in copper doped (3), even down to 0.1% Cu.

E.S.R. Spectra.—The polycrystalline e.s.r. spectrum of (1) is approximately axial [Figure 4(*c*)], while that of (2) [Figure

4(*d*)] is nearly isotropic with some evidence for exchange,[4] results that are surprising in view of the near alignment of both of the CuN_4O_2 chromophores in (1) and (2), if the local molecular axes [3] of the *cis* distorted-octahedral structure of Figure 1(*a*) are appropriate, with the *x* axis approximately

TABLE 1

The electronic reflectance spectra of some $[Cu(bipy)_2(OXO)]Y$ complexes (± 200 cm^{-1})

Y	Spectra E_2	E_1	Ref.
(*a*)			
NO_3 Complex (1)	14 600	9 500	3
BF_4 Complex (2)	15 000	9 500	this work
ClO_4	15 200	9 800	this work
NO_2	14 900	9 200	this work
	mean 14 900	9 500	
(*b*)			
$[Cu(bipy)_2(O_2CMe)][BF_4]$	15 150	10 860	19
$[Cu(bipy)_2(O_2CMe)][ClO_4]\cdot H_2O$	13 880	9 990	19
$[Cu(bipy)_2(O_2CH)][BF_4]$	14 360	10 200	20

(*c*) Tentative assignment of the electronic reflectance spectra of the $[Cu(bipy)_2(OXO)]Y$ complexes (square pyramidal 4 + 1 + 1*)

E_1 $d_{z^2} \longrightarrow d_{x^2-y^2}$
E_2 $d_{z^2}, d_{xz}, d_{yz} \longrightarrow d_{x^2-y^2}$

parallel to the crystallographic *b* axis (dihedral angle 3.3°). The e.s.r. spectra of copper doped (3) shows clear evidence for copper hyperfine [7] structure at low copper(II) concentrations, which is lost above 20% Cu, Figure 4(*a*). If the single-crystal *g* and *A* factors of copper doped (3) are measured in the directions used [3] for (1), namely, parallel to the *x*, *y*, and *z* axes of the *cis* distorted-octahedral structure

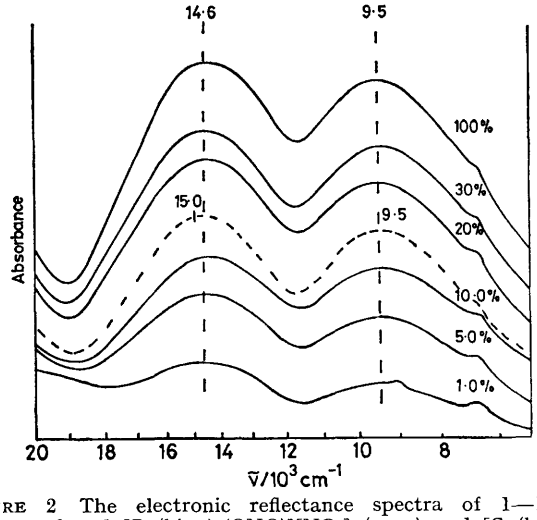

FIGURE 2 The electronic reflectance spectra of 1—100% copper doped $[Zn(bipy)_2(ONO)][NO_3]$ (——) and $[Cu(bipy)_2(ONO)][BF_4]$ (– – – –)

of Figure 1(*a*), the *g* and *A* values are essentially independent of the copper concentration, Table 2(*a*). The g_1 factor lies parallel to the N(1)–Zn–N(3) direction, and the g_2 factor lies parallel to the Zn–N(5) direction, approximately parallel [2] to the unique *b* axis (3.3°), Figure 6(*a*). When the *g* values are measured in these directions, g_2 parallel to the *b* axis and g_1 and g_3 in the *ac* plane in copper doped (3), the e.s.r. spectra involve *only* four copper hyperfine lines, consistent with the monoclinic crystal system, Figure 5(*b*) and (*c*). At liquid-nitrogen temperature only the g_1-factor shows any evidence of nitrogen hyperfine [Figure 4(*e*)]; all three *g* factors are virtually independent of temperature [Table 2(*c*)] but the copper hyperfine values, A_2 and A_3, do show a significant increase on decreasing the temperature. In these same directions the single-crystal *g* factors of (1), Table 2(*d*), are almost temperature independent. Despite the above, the single-crystal e.s.r. spectra of 1.0% copper doped (3) measured in the Zn,N(2),N(4),O(1),O(2)

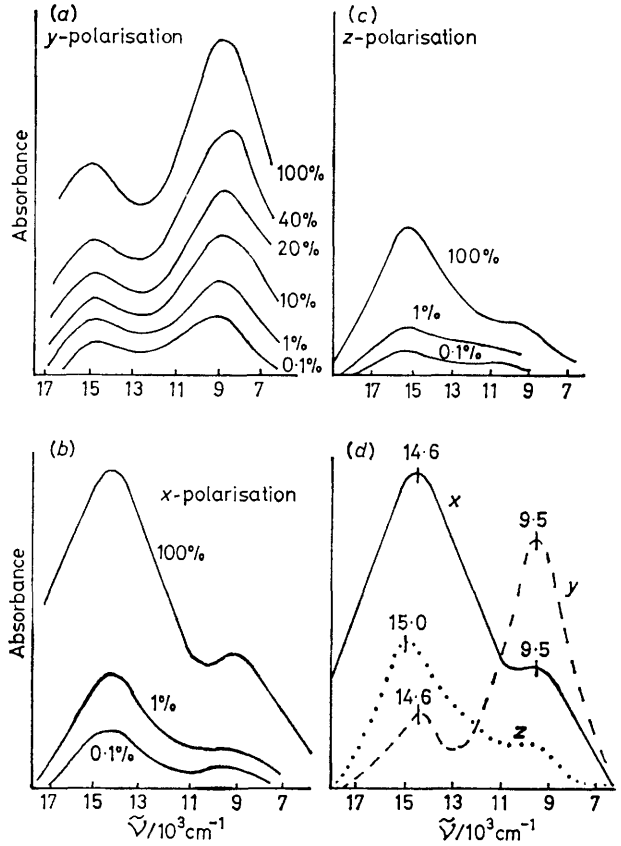

FIGURE 3 The polarised single-crystal electronic spectra of 0.1—100% copper doped $[Zn(bipy)_2(ONO)][NO_3]$: (*a*) *y*-polarisation, (*b*) *x*-polarisation, (*c*) *z*-polarisation, and (*d*) $[Cu(bipy)_2(ONO)][NO_3]$

plane, from the *b* axis to the *ac* plane shows clear evidence of two misaligned magnetic axes [Figure 5(*d*)], with the maximum *g* value measured at $\pm 40°$ to the *b* axis [Table 2(*e*)], which corresponds to the N(2)–Zn–O(1) and N(4)–Zn–O(2) directions of the $ZnN_2N'_2O_2$ chromophore, Figure 6(*a*). This misalignment is restricted to the Zn,N(4),-N(2),O(1),O(2) plane. At liquid-nitrogen temperature the highest *g* and *A* factors increase significantly and the intermediate *g* and *A* factors decrease relative to the room-temperature data, Table 2(*e*). Measurement of the single-crystal e.s.r. spectrum of (1) at the temperature of liquid nitrogen in the Cu,N(2),N(4),O(1),O(2) plane produced a single isotropic spectrum with no evidence for misaligned sites of Figure 5(*d*). The single-crystal e.s.r. spectrum of (2) yielded three crystal *g* factors, 2.020, 2.136, and 2.203, which correspond in magnitude and direction to the local molecular *g* factors [4] of (1), except that the intermediate *g* factor is lower.

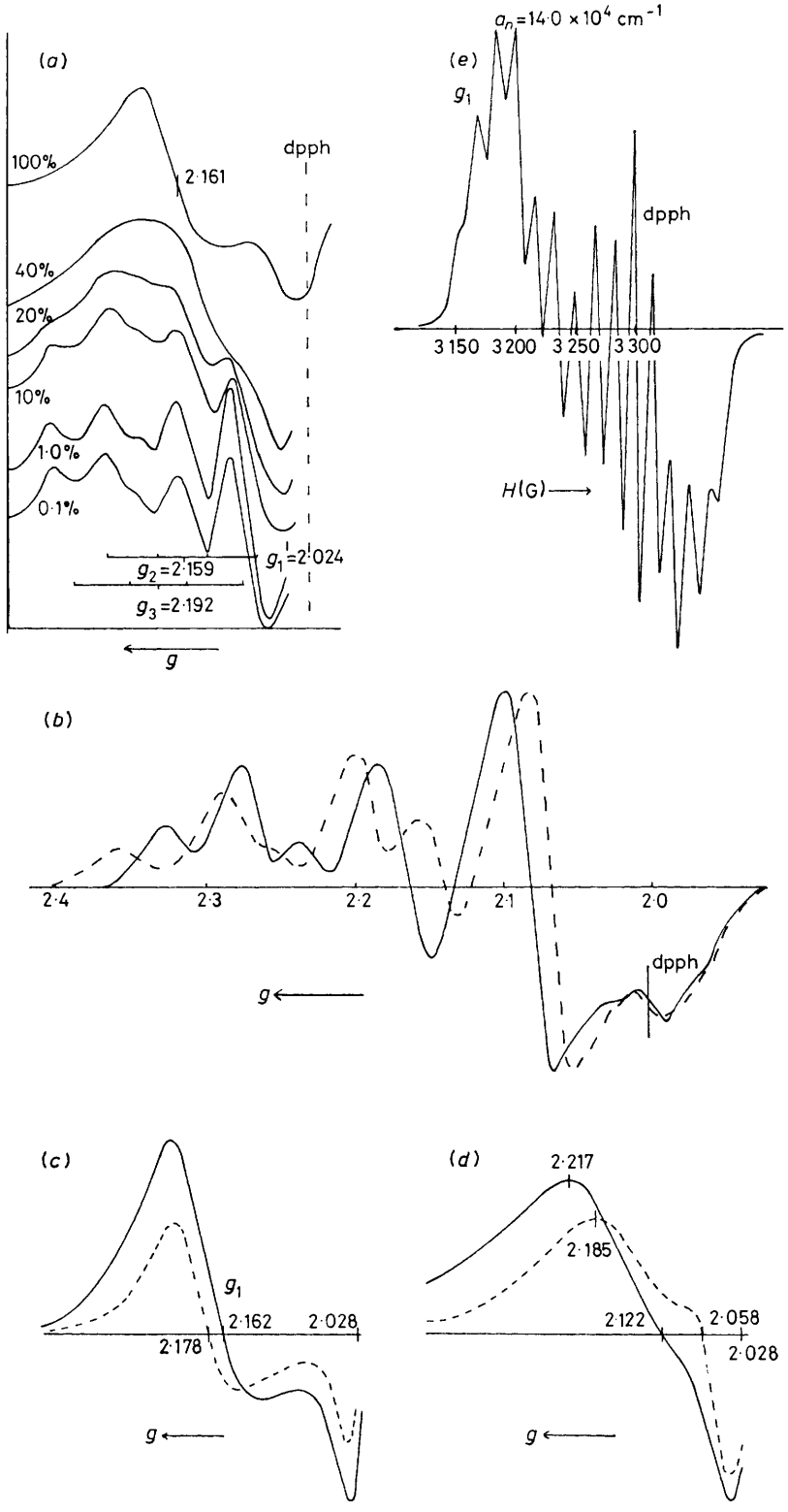

FIGURE 4 (*a*) The polycrystalline e.s.r. spectra of 0.1—100% copper doped $[Zn(bipy)_2(ONO)][NO_3]$ at room temperature (r.t.); (*b*) the polycrystalline e.s.r. of 0.1% copper doped $[Zn(bipy)_2(ONO)][NO_3]$ at r.t. (——) and at liquid-nitrogen temperature (l.t.) (– – – –); (*c*) the polycrystalline e.s.r. spectra of $[Cu(bipy)_2(ONO)][NO_3]$ at r.t. (——) and at l.t. (– – – –); (*d*) the polycrystalline e.s.r. spectra of $[Cu(bipy)_2(ONO)][BF_4]$ at r.t.(——) and at l.t. (– – – –); (*e*) the single-crystal e.s.r. spectra (g_1) of 0.1% copper doped $[Zn(bipy)_2(ONO)][NO_3]$ at l.t. dpph = Diphenylpicrylhydrazyl

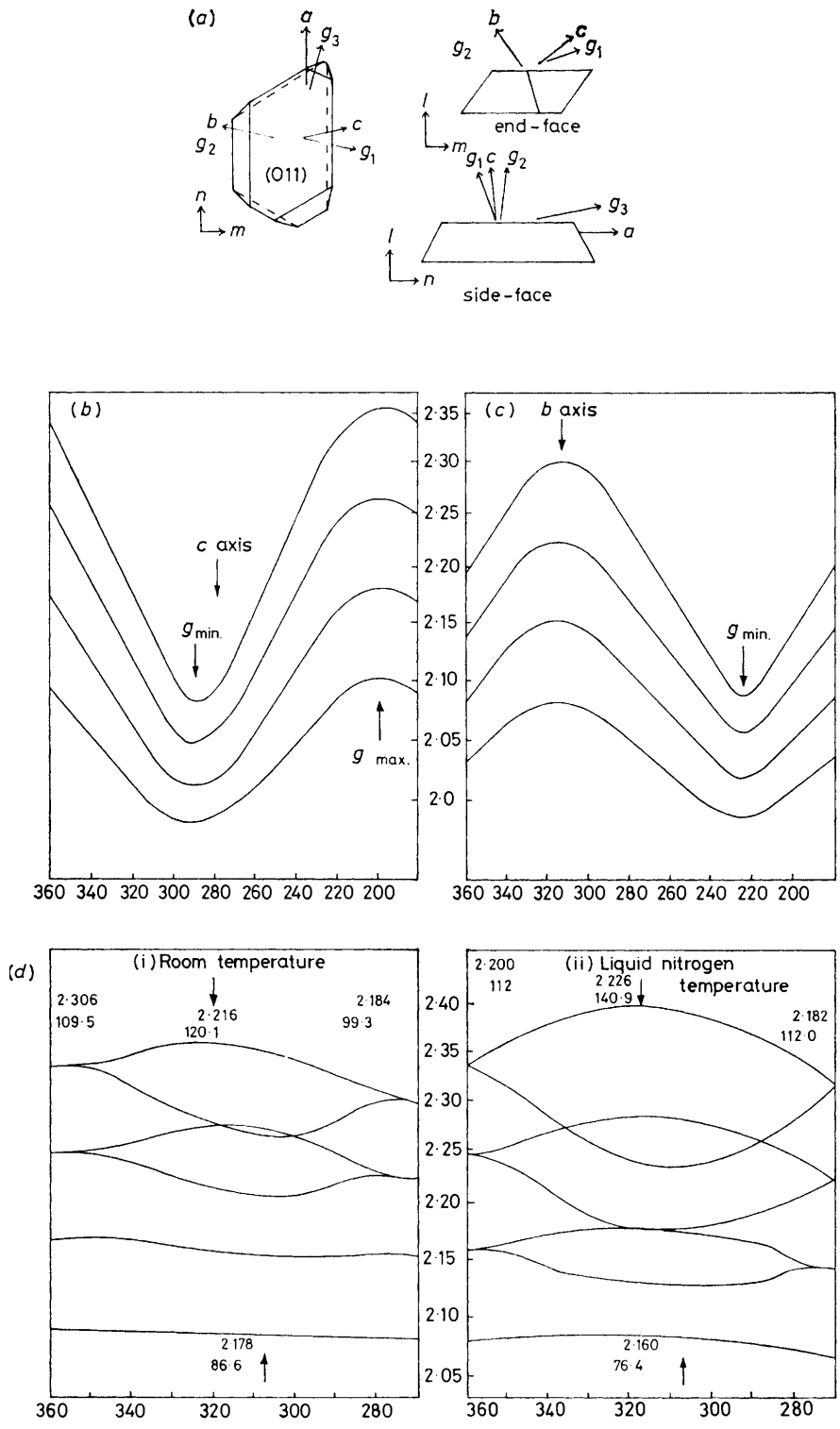

FIGURE 5 Copper doped $[Zn(bipy)_2(ONO)][NO_3]1$; [(*a*) 0.%(*b*)—(*d*) 1.0%: (*a*) crystal morphology, (*b*) *b* axis e.s.r. spectra, (*c*) $g_{min.}$ to *b* axis e.s.r. spectra, (*d*) $g_{max.}$ to *b* axis e.s.r. spectra, (i) at r.t. and (ii) at l.t.

DISCUSSION

Fluxional Model of the $CuN_2N'_2O_2$ *Chromophore.*—The crystallographic and electronic properties of the *cis* distorted-octahedral $CuN_2N'_2O_2$ chromophore in (1), (2), and copper(II) doped (3) are best rationalised in terms of a fluxional model of the $CuN_2N'_2O_2$ chromophore stereochemistry as originally proposed [8] for the copper doped $K_2[Zn(OH_2)_6][SO_4]_2$ system and more recently extended to a number of other copper doped systems.[9-16] All of these systems occur in crystals of lower than cubic symmetry and involve six-co-ordinate CuL_6 chromophores with non-equivalent ligands, which are subject to the pseudo-dynamic Jahn–Teller Effect.[17] Under the effect of the low crystal symmetry the observed CuL_6 chromophore stereochemistry at a given temperature is determined by the relative thermal populations of the three available potential energy Wells, each corresponding to an elongated rhombic octahedral stereochemistry misaligned in three mutually perpendicular directions related by the three-fold axis of the parent octahedron, Figure 7(*a*). In the $[Cu(bipy)_2(ONO)]^+$ cation, the potentially energy Wells I, II, and III involve elongation along the N(4)–Cu–O(2), N(2)–Cu–O(1), and N(1)–Cu–N(3) directions respectively, with the latter clearly of higher energy due to the restriction caused by the bite of the bipy ligands. The $CuN_2N'_2O_2$ structures of Wells I and II are equivalent due to the C_2 axis of symmetry of the *regular cis* distorted-octahedral structure, and represent the two alternative senses of distortion of the latter towards the distorted square-pyramidal (4 + 1 + 1*) type structure,[18] as recently reported for $[Cu(bipy)_2(O_2CMe)][ClO_4]\cdot H_2O$, $[Cu(bipy)_2(O_2CMe)][BF_4]$,[19] and $[Cu(bipy)_2(O_2CH)][BF_4]$ (4).[20] When only the lowest potential-energy Well I is occupied, a distorted square-pyramidal (4 + 1 + 1*) structure is observed as in (4) (see later), which is temperature independent. If the next lowest potential-energy Well II is low enough in energy ($\Delta E < kT$) and the potential-energy barrier B [Figure 7(*a*)] is also less than thermal energy ($kT = 200$ cm^{-1}), then partial thermal population of Well II will occur, with the thermal population Well I > Well II, and the observed structure will be a mean of the distorted square-pyramidal (4 + 1 + 1*) structures I and II, weighted according to their thermal population. In addition, the observed stereochemistry (and the associated e.s.r. spectra) will be temperature variable,[8-16] a result that has been confirmed by the recent low-temperature crystal structure of $[NH_4]_2[Cu(OH_2)_6][SO_4]_2$,[14] in which the elongated rhombic-octahedral stereochemistry of the room-temperature structure shows a marked increase in the elongation at *ca.* 150 K.

In (1) the near symmetrical *cis* distorted-octahedral structure requires near degenerate potential-energy Wells I and II with ΔE less than 200 cm^{-1}, so that the values ΔN = [Cu–N(4)] – [Cu–N(2)], 0.035 Å, and ΔO = [Cu–O(2)] – [Cu–O(1)], 0.111 Å, are both very small [1] and the thermal population of Well III is zero. In (2) the same potential-energy system applies, but the energy difference between Wells I and II is greater and the thermal population in Well I ≫ Well II, with consequent larger values [2] of ΔN and ΔO of 0.090 and 0.345 Å respectively. These ΔN and ΔO values of (1) and (2) respectively compare with the larger values observed in (4) of 0.154 and 0.671 Å respectively, which suggests that the population of Well II is very small and that the structure of (4) corresponds to an essentially static

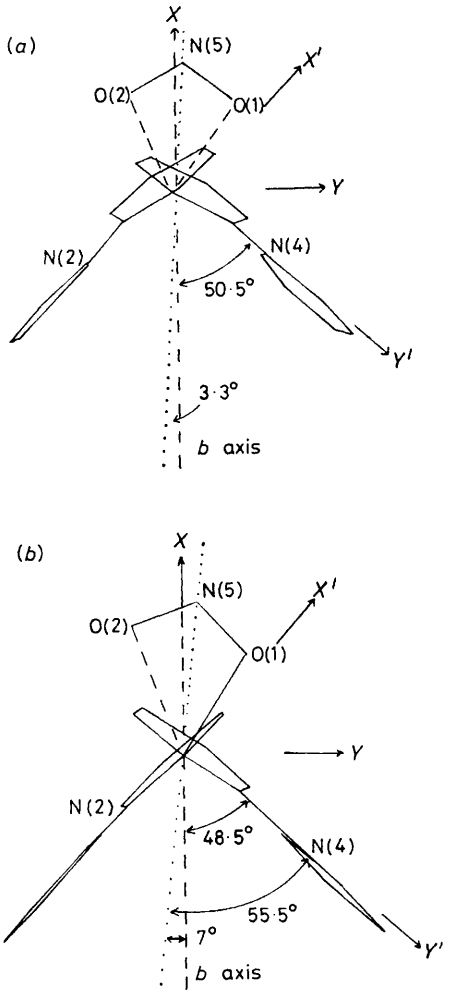

FIGURE 6 Crystallographic projections down the N(1)–N(3) direction of (*a*) $[Cu(bipy)_2(ONO)][NO_3]$, and (*b*) $[Cu(bipy)_2(ONO)][BF_4]$

distorted square-pyramidal (4 + 1 + 1*) structure, compared with the near equal population of Wells I and II in (1).

This two-dimensional fluxional model of (1) and (2) receives some support from the observation of relatively high and anisotropic thermal parameters associated with the O(1) and O(2) atoms [1,2,21] of (1) and (2).

E.S.R. Spectra.—The fluxional model predicts that the e.s.r. spectra would be temperature variable,[8-16] an effect that would be restricted to the Cu,N(2),N(4),-O(1),O(2) plane and would be at a maximum when measured along the N(2)–Cu–O(1) and N(4)–Cu–O(2) directions, the X' and Y' axes of Figure 6(*a*). As the

X' and Y' axes are then misaligned with respect to the b axis by *ca.* 40° in (1), this will produce a two-dimensional exchange coupling [4,11] in the e.s.r. spectrum, and explains the observation of the exchange type polycrystalline e.s.r. spectrum for (1) [Figure 4(*c*)] which only yields crystal g values measured in the X and Y directions of Figure 6(*a*). The relative insensitivity of the polycrystalline e.s.r. spectrum to decreasing temperature is then understandable, as g_1 is predicted [8] to be virtually temperature invariant, g_2 will decrease and g_3 increase with decreasing temperature; as the measured g values are a mean of g_2 and g_3, they would not be very temperature dependent, as is observed.

As (1) and (3) are as near isomorphous as a copper(II) and zinc(II) complex can be,[1,2] considering the d^9 and d^{10} electron configuration of these two ions respectively, the e.s.r. spectrum of the copper(II) doped complex (3) should also yield evidence [Figure 4(*b*)—(*d*)] for the fluxional model. In the 0.1 or 1.0% copper(II) doped (3) system, the full rotational single-crystal spectra yielded only four copper hyperfine lines in all directions in the *ac* plane [Figure 5(*b*)] and in the *ab* plane [Figure 5(*c*)], consistent with a single magnetic site aligned parallel to the *b* axis. But in the Zn,N(2),N(4),O(1),O(2) plane (parallel to the *b* axis and at 10° to the *c* axis), there is clear separation into more than four lines indicating the presence of two misaligned magnetic sites orientated at 40° to the *b* axis, Figure 5(*d*). This confirms that the local molecular axes of the $CuN_2N'_2O_2$ doped complex (3) system correspond with the z axis of Figure 1(*a*) and the X' and Y' axes of Figure 6(*a*), with the $X'Y'$ axes misaligned with respect to the *b* axis. Consequently, the local molecular g and A factors correspond with the z, x', and y' axes of Figure 1(*a*), and the data are summarised in Table 2(*e*). Figure 5(*d*) shows a significant temperature effect, and yields the characteristic data consistent with a two-dimensional fluxional $CuN_2N'_2O_2$ chromophore [8-16] with g_3 and A_3 increasing, g_2 and A_2 decreasing, and g_1 and A_1 remaining temperature invariant, with decreasing temperature. Results that contrast with the temperature invariance of the g factors when measured along the *b* axis, and in the *ac* plane for both the concentrated [3] [Table 2(*d*)] and the dilute system, Table 2(*c*).

The room-temperature g values of 1.0% copper doped (3) have an R value [4,16] $[(g_2 - g_1)/(g_3 - g_2)]$ of 4.026 consistent with an approximate d_{z^2} ground state, but as these local molecular g values correspond to a fluxional copper stereochemistry, they only relate to the average *cis* distorted-octahedral structure. The R value decreases to 2.061 at the temperature of liquid nitrogen, consistent with a more elongated tetragonal-octahedral stereochemistry, but still consistent with an approximate d_{z^2} ground state.[4,16]

Despite the clear temperature effect on the e.s.r. of 0.1—1.0% copper doped (3) [Figure 4(*b*) and 5(*d*)], the effect on (1) is hardly significant, Figure 4(*c*), and Table 2(*d*), and the single-crystal rotation spectra of (1) measured in the Cu,N(2),N(4),O(1),O(2) plane showed *no* evidence for splitting into two bands in any direction. Thus (1) displays no evidence for the fluxional model in the low-temperature e.s.r. spectrum.

The single-crystal e.s.r. spectrum of (2) yielded three crystal g factors, 2.020, 2.136, and 2.203, and although these correspond in magnitude to the local molecular g factors [4] of (1), except that the highest and intermediate values are lower, they are not necessarily local molecular g factors, as misalignment of the local molecular axes [2] of (2) is present [Figure 6(*b*)] and a fluxional description of the local molecular geometry is relevant, as suggested by comparison of the structure of (1) and (2). Due to this uncertainty no significant use of the single-crystal g values of (2) can be made, especially as the corresponding $[Zn(bipy)_2(ONO)][BF_4]$ complex proved not to be

TABLE 2

Electron spin resonance data ; Cu hyperfine ($\times 10^4$ cm^{-1})

(*a*) The g and A values for 0.1—100% copper doped $[Zn(bipy)_2(ONO)][NO_3]$ as measured in the directions used for (1)

% Cu	g_z	g_x	g_y	A_z *	A_x	A_y
0.1	2.024	2.159	2.192	*ca.* 30	93.2	106.1
1.0	2.025	2.165	2.197	*ca.* 30	91.7	105.7
10.0	2.027	2.168	2.200		91.7	106.4
40.0	2.028	2.166	2.197			
100.0	2.025	2.165	2.196			

(*b*) Angular directions (°) of the g factors and zinc–nitrogen directions in 1.0% copper doped $[Zn(bipy)_2(ONO)][NO_3]$ with respect to the directions l, m, and n of Figure 5(*a*), as measured in the directions used for (1) [a]

	g_1 (2.025)	g_2 (2.165)	g_3 (2.196)
l	69.6	42.7	54.4
m	76.7	132.0	45.0
n	24.7	96.4	113.7
	N(1)–Zn–N(3)	Zn–N(2)	Zn–N(4)
l	70.0	5.0	85.0
m	70.0	78.0	170.0
n	20.0	95.0	85.0

(*c*) Single crystal g, A_{Cu}, and A_N values at room and liquid-nitrogen temperature for 1.0% copper doped $[Zn(bipy)_2(ONO)][NO_3]$, measured in the directions used for (1) [a]

Temp.			A_{Cu}(average)	A_N(average)	Number of peaks
r.t.	g_1	2.024	30		
l.t.	g_1	2.024		16.7	14
r.t.	g_2	2.168	91.6		
l.t.	g_2	2.169	103.6	6.3	5—6
r.t.	g_3	2.196	104.9		
l.t.	g_3	2.192	112.0	7.2	5

(*d*) The single-crystal e.s.r. spectra of $[Cu(bipy)_2(ONO)][NO_3]$ measured at room temperature and at liquid-nitrogen temperature, as measured in the directions used for (1) [a]

	g_1	g_2	g_3	R
r.t.	2.019	2.174	2.205	4.39
l.t.	2.029	2.175	2.200	5.44

(*e*) The g and A values for the 1.0% copper doped $[Zn(bipy)_2(ONO)][NO_3]$ measured along the approximate N(4)–Cu–O(2) directions, ±40° to the *b* axis, from Figure 5(*d*)

	g_3	A_3	g_2	A_2	g_1	A_1	R [b]
r.t.	2.216	120.1	2.178	86.6	2.025	*ca.* 30	4.206
l.t.	2.226	140.9	2.160	76.4	2.024		2.061

* Only approximate, as linewidth was broader than hyperfine splitting.

[a] See ref. 3.

[b] $R = (g_2 - g_1)/(g_3 - g_2)$.

isomorphous with (2) and unsuitable for use as a diamagnetic host lattice.

Electronic Spectra.—In view of the different geometries of (1) and (2) [Figure 1(*a*) and (*b*)], it is surprising that the electronic spectra of (1) and (2) (Figure 2) are so closely comparable (9 500, 14 600 and 9 500, 15 000 cm^{-1} respectively), a similarity that has also been noted earlier in $[Cu(bipy)_2(O_2CMe)][BF_4]$ (5),[19] and $[Cu(bipy)_2(O_2CMe)][ClO_4]$ (6),[19] and also with $[Cu(bipy)_2(O_2CH)][BF_4]$ (4),[20] Table 1(*b*). As all five complexes have pseudo *cis* distorted-octahedral structures, with increasing distortions towards square pyramidal, a measure of this distortion is the increasing asymmetry in bonding of the OXO^- anion [where OXO^- is ONO^- in (1) and (2), $CH_3CO_2^-$ in (5) and (6), and HCO_2^- in (4)] which is measured by the difference in the ΔN and ΔO values, see earlier. If the electronic energies (E_1 and E_2) are plotted against ΔO [Figure 9], there is only a slight change in both energies with increasing ΔO, E_1 increases slightly (*ca.* 400 cm^{-1}) and E_2 decreases slightly (*ca.* 200 cm^{-1}). The lack of change in E with ΔO is consistent with the above fluxional model for (1) and (2). This independence of E_1 and E_2 of ΔO is consistent with a two-dimensional fluxional model, as the electronic transitions (10^{-15} s) represent the local molecular structure in the extreme static distorted square-pyramidal (4 + 1 + 1*) structures of Wells I and II, which involve the *same* local $CuN_2N'_2O_2$ chromophore structure, but with the local elongation axes misaligned by 90°. Consequently, the electronic spectra are independent of the relative thermal population of the Wells I and II, but only sensitive to the precise geometry of the static $CuN_2N'_2O_2$ chromophore in a given lattice. In these cation distortion isomers of (1) and (2), the small differences in the observed E_1 and E_2 energies arise from small differences in the lattice packing factors, which are much less effective in influencing the geometry of these six-co-ordinate chromophores, than they are in influencing the five-co-ordinate geometry of the $[Cu(bipy)_2Cl]^+$ cation in its cation distortion isomers.[22]

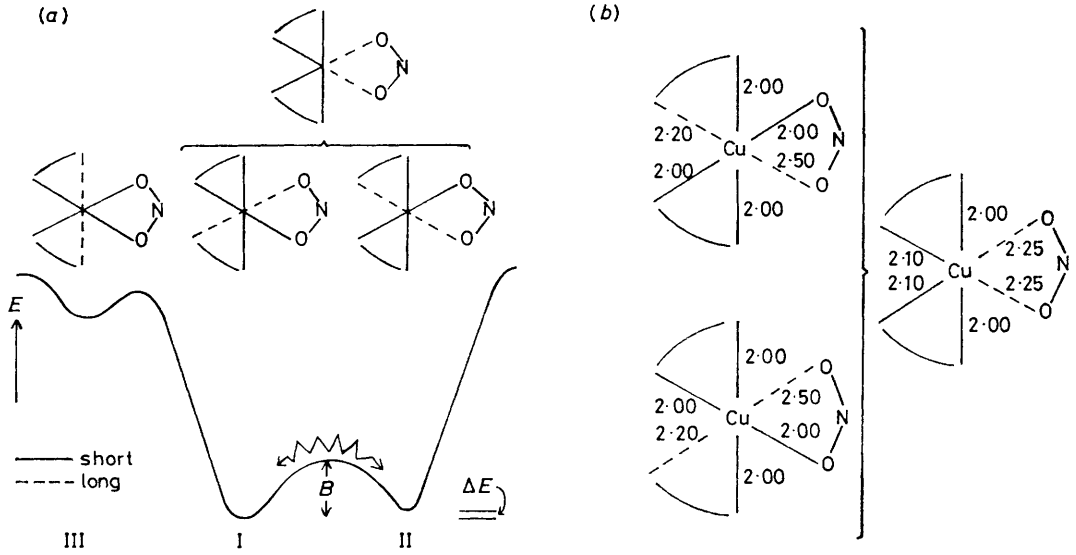

FIGURE 7 $[Cu(bipy)_2(ONO)]Y$: (*a*) static disorder model, (*b*) fluxional disorder model

TABLE 3

Unit-cell data for $[Zn(bipy)_2(ONO)][NO_3]$ (3) and $[Cu(bipy)_2(ONO)][NO_3]$ (1) *

	Complex (3)	Complex (1)
a/Å	11.27(5)	11.101
b/Å	11.93(5)	12.058
c/Å	15.49(5)	15.383
β/°	101.2(2)	99.17

* Both space group $P2_1/n$.

If the two-dimensional fluxional model of (1) involving almost equal thermal population of Wells I and II is correct, it is then surprising that the polarised single-crystal electronic spectra of (1) show such marked polarisation, Figure 3(*d*). As the model involves ±40° misalignment of the *x'* and *y'* directions of Figure 1(*a*), there is a surprising difference between the *x*- and *y*-polarised spectrum. Equally surprising is that the *z*-polarised spectrum, which is still a unique direction in the fluxional model, is closely comparable to the *x*-polarised spectrum, and only differs in its relative intensity. Nevertheless, as the polarised single-crystal spectra of (1) were assigned with respect to the *x*, *y*, and *z* axes of Figure 1(*a*), this assignment is clearly no longer valid in view of the ±40° misalignment present, plus a local molecular $CuN_2N'_2O_2$ structure that is so fluxional that Wells I and II are almost equally populated. The comparable polarisation of the 0.1—100% copper(II) doped (3) system [Figure 3(*a*)—(*d*)] is then also understandable as the spectra were all measured with respect to the *x*, *y*, and *z* axes, and not to the *x'*, *y'*, and *z* axes, but for the reasons given above, cannot be used to establish even a tentative one-electron orbital sequence. Nevertheless, the distorted square-pyramidal (4 + 1 + 1*) structure of (2) is comparable to structures of

$[Cu(dien)_2(O_2CH)][HCO_2]$, and suggests a comparable assignment [23] of the one-electron orbital sequence, namely $d_{x^2-y^2} > d_{z^2} > d_{xy} > d_{xz} \approx d_{yz}$, Table 1(*c*).

The Nature of the cis *Distorted-octahedral Structure.*—The structures of the CuN_4O_2 chromophores of (1) and (2) [Figure 1(*a*) and (*b*)] both involve a pseudo *cis* distorted-octahedral arrangement of the ligands; while (1) has an almost symmetrical C_2 symmetry,[1] that of (2) has a clear distortion towards a (4 + 1 + 1*) type structure,[18] with the elongation along the N(4)–Cu–O(2) direction.[2] Thus (1) and (2) represent clear cation distortion isomers [24] of the $[Cu(bipy)_2(ONO)]^+$ cation, which represent two separate points on the structural pathway [25] connecting the higher energy *cis* distorted-octahedral structure to the square-pyramidal distorted (4 + 1 + 1*) structure (Figure 8; see ref. 2 for discussion). While the structure of (1) is more closely related to the regular *cis* distorted-octahedral structure, that of (2) corresponds to an intermediate form of the square-pyramidal (4 + 1 + 1*) structure. As there are two possible routes to the latter type of distortion, *via* route E or F of Figure 8, it could be argued that the pseudo *cis* distorted-octahedral structure arises from an appropriate weighted mixture of the two misaligned forms of the two *static* (4 + 1 + 1*) structures, Figure 7(*b*). As the dilute copper doped (3) system identifies the two magnetically equivalent sites, misaligned with respect to the unique *b* axis of this monoclinic system, a disordered structure is possible, but there is no reason why static disorder of the local molecular structure should be so temperature variable as required for the two-dimensional fluxional model.[8–16] For this reason the near *cis* distorted-octahedral structure of (1) is not considered to be a genuine *static* stereochemistry of the copper(II) ion, but to arise as a consequence of the pseudo-dynamic Jahn–Teller Effect [17] generating a two-dimensional fluxional model [8–16] involving a *static* distorted square-pyramidal (4 + 1 + 1*) structure, with nearly equal thermal population of two lowest potential Wells I and II, which are thermally related. Consequently, the structures of (1) and, to a lesser extent, (2) are not genuine static stereochemistries of the copper(II) ion, but arise as a consequence of the two-dimensional fluxional model (pseudo-dynamic Jahn–Teller Effect), and are best referred to as pseudo *cis* distorted-octahedral structures. This term has been previously suggested for the compressed tetragonal-octahedral structures of $Rb_2[PbCu(NO_2)_6]$,[10] $Cs_2[PbCu(NO_2)_6]$,[11] and $[Cu(dien)_2(NO_3)_2]$,[14] which also arise as a consequence of the two-dimensional fluxional CuN_6 chromophore present in these complexes.[16]

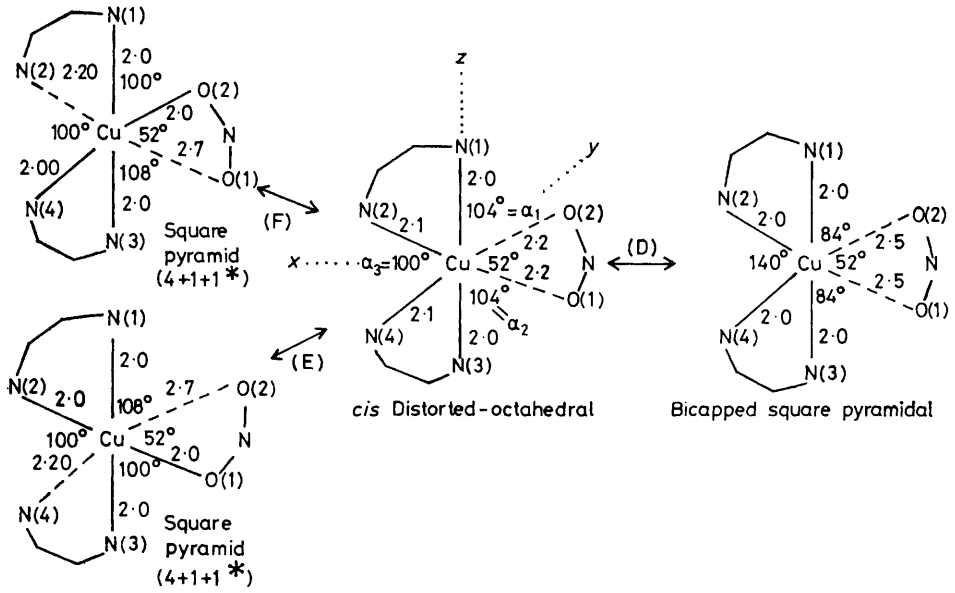

FIGURE 8 The structural pathways for the $CuN_2N'_2OO'$ chromophore of the $[Cu(chelate)_2(ONO)]^+$ cation for distortion from regular *cis* distorted-octahedral to distorted square pyramidal (route E and F) and to bicapped square pyramidal (route D)

It is unfortunate that the e.s.r. spectrum of (1) shows no significant variation with temperature, down to liquid-nitrogen temperature, as it suggests that temperatures down to liquid-helium temperature will be required to reveal this e.s.r. evidence for (1). It also implies that a crystal structure determination of (1) below that of liquid-nitrogen temperature will be necessary to reveal the two-dimensional fluxional behaviour of (1).

The Origin of the Pseudo cis *Distorted-octahedral Stereochemistry.*—It has been suggested earlier [3] that the origin of the *cis* distorted-octahedral stereochemistry was due to one of the components, *B* (or S_{1a}[26]) (Figure 10), of C_2 symmetry, of the doubly degenerate *E* modes of vibration of a regular tris(chelate)copper(II) complex of D_3 symmetry.[26] In a tris(chelate)copper(II) complex involving two equivalent and one non-equivalent chelate ligand, such as $[Cu(bipy)_2(OXO)]Y$, the magnitude of this distortion is enhanced to give a clear *cis*

distorted-octahedral stereochemistry, but as this distortion also occurs in the corresponding zinc(II) complex,[2] the distortion cannot be Jahn-Teller in origin and must originate in the S_{1a} mode of vibration. As the *cis* distortion is not symmetrical in either (1) or (2), the final

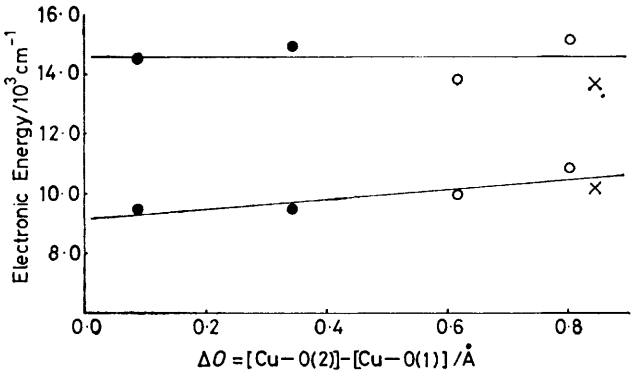

FIGURE 9 Plot of the electronic energies E_1 and E_2 *versus* ΔO = [Cu–O(2)] – [Cu–O(1)] for [Cu(bipy)$_2$(OXO)]Y: OXO = ONO$^-$ (●), O_2CMe^- (○), O_2CH^- (×)

stereochemistry must originate from a linear combination of the S_{1a} and S_{2a} modes of vibration, with the contribution of S_{2a} greater in (2). The greater N(4)–O(2) distortion of (2) than (1) is facilitated by the preferred prolate ellipsoidal shape of the copper(II) ion,[4] while the lower distortion of (3) relates to the spherical symmetry of the d^{10} configuration of the zinc(II) ion.

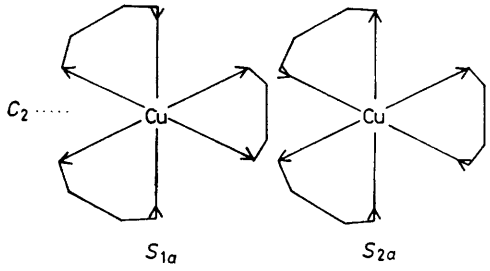

FIGURE 10 The normal modes of vibration of *E* symmetry of a regular tris(chelate)copper(II) complex

Non-co-operative Jahn–Teller Effect.—The space groups [1,2] of both (1) and (3) are isomorphous ($P2_1/n$ with closely comparable unit cell parameters, Table 3); it is then significant that the electronic energies (Figures 2 and 3) and the *g* factors (Figure 4) of copper doped (3) are independent of the percentage doping, and suggests that the stereochemistry of the doped CuN_4O_2 is comparable to the structure of this chromophore in the pure complex (1),[1] and is not related to the structure of the ZnN_4O_2 chromophore [2] in this near isomorphous lattice. Thus, despite the near isostructural nature of the CuN_4O_2 and ZnN_4O_2 chromophores, the local structure of the CuN_4O_2 chromophore when doped in (3) should not be equated with the local structure of the ZnN_4O_2 host lattice.[27] It also suggests that the stereochemistry of the CuN_4O_2 chromophore in (1) is, in *this* complex, independent of neighbouring copper(II) ions in the lattice, and not dependent on, as required by the ' Co-operative Jahn–Teller Effect ',[11] a structural situation that is best described as the Non-co-operative Jahn–Teller Effect.[6,28]

We acknowledge the award of Department of Education Grants (to A. W., B. W., and W. F.), and of a Senior Demonstratorship, U.C.C. (to S. T.).

[0/1957 *Received*, 19*th December*, 1980]

REFERENCES

[1] F. S. Stephens, *J. Chem. Soc. A*, 1969, 1248.
[2] A. Walsh, B. Walsh, B. Murphy, and B. J. Hathaway, *Acta Crystallogr.*, in the press.
[3] I. M. Procter, B. J. Hathaway, D. E. Billing, R. Dudley, and P. Nicholls, *J. Chem. Soc. A*, 1969, 1192.
[4] B. J. Hathaway and D. E. Billing, *Coord. Chem. Rev.*, 1970, **5**, 1.
[5] B. J. Hathaway, P. Nicholls, and D. Barnard, *Spectrovision*, 1969, **22**, 4.
[6] M. Duggan, M. Horgan, J. Mullane, P. C. Power, N. Ray, A. Walsh, and B. J. Hathaway, *Inorg. Nucl. Chem. Lett.*, 1980, **16**, 407.
[7] B. A. Goodman and J. B. Raynor, *Adv. Inorg. Chem. Radiochem.*, 1970, **13**, 135.
[8] D. Getz and B. L. Silver, *J. Chem. Phys.*, 1974, **61**, 638.
[9] J. Pradilla-Sorzano and J. P. Fackler, *Inorg. Chem.*, 1973, **12**, 1182.
[10] S. Takagi, M. D. Joeston, and P. G. Lenhert, *J. Am. Chem. Soc.*, 1975, **97**, 444.
[11] D. Reinen and C. Friebel, *Struct. Bonding*, 1979, **37**, 1.
[12] B. Walsh and B. J. Hathaway, *J. Chem. Soc., Dalton Trans.*, 1980, 681.
[13] M. Duggan, B. J. Hathaway, and J. Mullane, *J. Chem. Soc., Dalton Trans.*, 1980, 690.
[14] M. Duggan, A. Murphy, and B. J. Hathaway, *Inorg. Nucl. Chem. Lett.*, 1979, **15**, 103.
[15] I. Bertini, D. Gatteschi, and A. Scozzafava, *Coord. Chem. Rev.*, 1979, **27**, 67.
[16] B. J. Hathaway, M. Duggan, A. Murphy, J. Mullane, C. Power, A. Walsh, and B. Walsh, *Coord. Chem. Rev.*, 1981, **36**, 267.
[17] I. B. Bersuker, *Coord. Chem. Rev.*, 1975, **14**, 357.
[18] B. J. Hathaway, *Struct. Bonding*, 1973, **14**, 49.
[19] B. J. Hathaway, N. Ray, D. Kennedy, N. O'Brien, and B. Murphy, *Acta Crystallogr., Sect. B.*, 1980, **36**, 1371.
[20] W. Fitzgerald and B. J. Hathaway, *J. Chem. Soc., Dalton Trans.*, 1981, 567.
[21] C. J. Simmons, K. Seff, F. Clifford, and B. J. Hathaway, *Acta Crystallogr.*, submitted for publication; C. J. Simmons, M. Lundeen, P. W. Payne, K. Seff, and B. J. Hathaway, *Inorg. Chem.*, submitted for publication.
[22] D. Harrison, D. Kennedy, and B. J. Hathaway, *Inorg. Nucl. Chem. Lett.*, 1981, **17**, 87; *J. Chem. Soc., Dalton Trans.*, 1981, 1556.
[23] M. J. Bew, R. J. Dudley, R. J. Fereday, B. J. Hathaway, and R. C. Slade, *J. Chem. Soc. A*, 1971, 1437.
[24] N. Ray, L. Hulett, R. Sheahan, and B. J. Hathaway, *Inorg. Nucl. Chem. Lett.*, 1978, **14**, 305.
[25] H. G. Burgi, *Angew. Chem. Int. Ed.*, 1975, **14**, 460; E. L. Muetterties and L. T. Guggenberger, *J. Am. Chem. Soc.*, 1974, **96**, 1748; J. D. Dunitz, '*X*-Ray Analysis and the Structure of Organic Molecules,' Cornell University Press, London, 1979; J. D. Dunitz, at the J. M. Robertson Symposium, Glasgow, September 1980; P. Murray-Rust and J. Murray-Rust, *Acta Crystallogr., Sect. A*, 1975, **31**, 564.
[26] H. G. Burgi, personal communication.
[27] A. Bencini, I. Bertini, D. Gatteschi, and A. Scozzafava, *Inorg. Chem.*, 1978, **17**, 3194.
[28] M. R. Lowrey and J. R. Pilbrow, *J. Phys. C*, 1977, **10**, 439.